coatings

MDPI

Article

Cutting Performance of Multicomponent AlTiZrN-Coated Cemented Carbide (YG8) Tools during Milling of High-Chromium Cast Iron

Hu Yang, Renxin Wang, Ziming Guo, Rongchuan Lin *, Shasha Wei * and Jianchun Weng *

College of Marine Equipment and Mechanical Engineering, Jimei University, Xiamen 361021, China; yh980609@163.com (H.Y.); wrx15828950828@163.com (R.W.); 15238021625@139.com (Z.G.)
* Correspondence: rongchuan@jmu.edu.cn (R.L.); 200461000025@jmu.edu.cn (S.W.); gingerwjc@163.com (J.W.)

Abstract: In order to improve the cutting performance of cemented-carbide (YG8) tools during the milling of high-chromium cast iron, AlTiZrN coating was deposited on the surface of YG8 samples and milling tools by physical vapor deposition (PVD) technology. The micromorphology and mechanical properties of the coating were studied by the experimental method, and the cutting performance of the coated tools was tested by a milling machining center. The results show that the AlTiZrN coating presents the face-centered cubic (fcc) structure of TiN. The average microhardness is 3887 $HV_{0.05}$. The bonding strength between the coating and the substrate meets the standard HF3 and is up to the requirements. The coefficient of friction (COF) of the coating is about 0.32. AlTiZrN coating can significantly improve the life of cemented-carbide tools. At cutting speeds of 85, 105, and 125 mm/min, the lives of the AlTiZrN-coated tools increased by 20.7%, 22.4%, and 35.2%, respectively, compared with the uncoated tools. Under the same cutting condition, AlTiZrN-coated tools have better cutting and chip-breaking performance than uncoated tools. With the increase in cutting speed, the workpiece chips produced by AlTiZrN-coated tools are smaller and more uniform, and the scratches on the machined surface are smoother. Therefore, at higher cutting speeds, AlTiZrN-coated tools have more advantages in life and cutting performance than that of uncoated tools. During the cutting process, the wear mechanisms of the AlTiZrN-coated tools mainly included friction, oxidation, and bonding, while oxidation and bonding wear were the main wear mechanisms in the later stage of wear.

Keywords: physical vapor deposition; AlTiZrN coating; milling; cutting performance; wear mechanism

Citation: Yang, H.; Wang, R.; Guo, Z.; Lin, R.; Wei, S.; Weng, J. Cutting Performance of Multicomponent AlTiZrN-Coated Cemented Carbide (YG8) Tools during Milling of High-Chromium Cast Iron. *Coatings* **2022**, *12*, 686. https://doi.org/10.3390/coatings12050686

Academic Editor: Stefano Caporali

Received: 24 April 2022
Accepted: 13 May 2022
Published: 16 May 2022

1. Introduction

As the most widely used casting metal material in modern industrial production, cast iron plays an important role in machinery manufacturing, metallurgy and mining industry, petrochemical industry, transportation, and national defense industry. With the continuous development of industry, the production of high hardness cast iron gradually replaces ordinary cast iron. As a kind of high hardness cast iron, high-chromium cast iron has developed into the third generation of wear-resistant materials. At present, high-chromium cast iron is widely used in cement, electric power, mining, and other industries [1]. How to improve the processing efficiency of high-chromium cast iron has become a problem that tool manufacturers need to consider at present. Common tools for cutting high-chromium cast iron include cemented-carbide tools [2,3] and Cubic Boron Nitride (CBN) tools [4–6]. However, cemented-carbide tools have low hardness and quick wear, which are suitable for small-scale production of high-chromium cast iron. CBN tools are recommended for large-scale processing [7]. However, CBN tools have stringent requirements on the environment and high costs. In order to improve the cutting performance of cemented-carbide tools, tool manufacturers gradually rely on coating technology [8].

The coating technology of cutting tools can be divided into chemical vapor deposition (CVD) technology and physical vapor deposition (PVD) technology. CVD technology is widely used in the surface treatment of cemented-carbide indexable tools. TiCN and thick film Al_2O_3 coating of medium temperature CVD can effectively improve the wear resistance of tools [9–12]. However, CVD coating technology also has defects, such as high treatment temperature and serious environmental pollution. Therefore, the development of PVD technology began to attract the attention of scientists. Wei, Adri á N, Alain, and others [13–17] studied different types of wear-resistant PVD coatings, such as TiN, AlTiN, and AlCrN, which significantly improved the life and cutting performance of tools. Elisangela, Grigoriev, Zheng, and others [18–21] studied various lubricating coatings, such as DLC, which greatly improved the wear resistance of tools. Along with the changing application environment of cutting tools, conventional PVD coatings cannot meet the demands, so it is necessary to develop more kinds of wear-resistant coatings. As a metal element, zirconium (Zr) has the characteristics of corrosion resistance, a high melting point, high hardness, high-temperature resistance, and easy extension, among others. The preparation of PVD coating with Zr element has become a hot research topic at present. The common coatings include ZrN, TiZrN, etc. [22–25]. However, few people have studied the application of the AlTiZrN coating on cutting tools.

As a common tool material, cemented-carbide YG8 can be used to cut cast iron, non-ferrous metals, and other materials. However, YG8 can only be suitable for slow cutting because of its poor heat resistance and wear resistance. In order to improve the performance of YG8 tools in the high-speed cutting of high-chromium cast iron, the multicomponent AlTiZrN coating was prepared on the surface of cemented-carbide YG8 samples and tools by PVD technology. The properties of the coating, along with the cutting performance and wear mechanisms of the coated tools, were studied so as to provide some reference for the development of multicomponent coating on cemented-carbide tools in the future.

2. Experimental Methods

AlTiZrN coating was deposited on the YG8 samples (30 mm × 7 mm × 6 mm) and YG8 welding tools by PVD equipment. The chemical composition and mechanical properties of YG8 are listed in Tables 1 and 2, respectively. In order to ensure the smoothness of the substrate and prevent the coating from peeling off due to impurities such as burrs, the samples should be polished by a polishing machine, and the oil stains on the surface of the samples and tools should be removed with a high-pressure steam gun before the coating deposition, and then put them into an ultrasonic cleaner for cleaning so that the surface of the samples can be smoother.

Table 1. Chemical composition of YG8 (wt.%).

Brand	Chemical Composition	
	WC	Co
YG8	92	8

Table 2. Physical and mechanical properties of YG8.

Brand	Physical and Mechanical Properties				
	Hardness (HRA)	Flexural Strength/MPa	Compressive Strength/MPa	Modulus of Elasticity/GPa	Thermal Conductivity/(W/mK)
YG8	89	1500	4470	600~610	75.36

The coating equipment was imported from Italy (ICS-S800, ICS, Milan, Italy). The deposition of the AlTiZrN coating requires an AlTi target (the percentage of the Al and Ti is 67:33) and a Zr target (the purity is 99.99%). The deposition process of the coating was as follows: vacuumizing the chamber to 0.5 Pa, heating the working temperature to

450 °C, introducing Ar gas, and cleaning the sample's surface by ion etching for 20 min. After the etching was completed, the current on the target was alternately changed in the N_2 environment to prepare the multicomponent AlTiZrN coating.

The morphology and chemical composition of the coating were characterized by a scanning electron microscope (ZEISS, Jena, Germany) equipped with energy-dispersive X-ray spectroscopy (EDS). X-ray diffraction (XRD, Bruker D8 advance, Karlsruhe, Germany) was used to analyze the phase structure, and the parameters were set as follows: scanning range was 20~90°, scanning speed was 3°/min, and scanning step was 0.02°. The microhardness of the coating was continuously measured by a Vickers hardness tester (Falcon511, Selfkant, The Netherlands) on the surface of the samples. In order to reduce error and ensure the accuracy of data, five effective values were measured and averaged. The indentation method was used to measure the bonding strength between the coating and the substrate with a Rockwell hardness tester (HRS-150, Rockwell, Shanghai, China). The applied load was 150 kg, and the duration was 5 s. The indentation morphology characteristics were observed under the optical microscope (VK-X1000, Keyence, Shanghai, China) and compared with the standard DB32/T 2945-2016 to judge whether the bonding strength was qualified. The coefficient of friction (COF) of the coating was tested by friction and wear tester (MM-2HB, HengXu, Jinan, China), and the test force was set to 20 N. The material of the friction ring was #45 steel; the size was φ40 × 10 mm, the rotating speed was 400 r/min, and the friction and wear time was 30 min.

The milling test was conducted by a Qifa Machinery Vertical CNC Milling Machine Center (VH-850L3, Qifa, Taizhong, Taiwan), as shown in Figure 1. The high-chromium cast iron KmTBCr12 was used as workpiece material; the composition of KmTBCr12 is listed in Table 3. The tool geometry and milling parameters are shown in Table 4. This study adopted the method of forward-milling. Because the cutting speed has a significant impact on the life of the tool, according to the characteristics of the machining center of the milling machine, the cutting speeds were set as 85, 105, and 125 mm/min, respectively. The cutting depth was kept at 0.2 mm, and the feed rate was kept at 0.2 mm/r. All the milling tests were paused at each interval cutting length of 3 cm, and the real-time flank wear of coated tools was measured via an optical microscope. Generally, average flank wear of 0.3 mm is designated as the failure standard. The workpiece processed in this paper belongs to difficult cutting materials, and the diameter of the cemented-carbide milling tool is small. In order to ensure the machining quality of the workpiece, average flank wear of 0.1 mm was assigned as the failure standard.

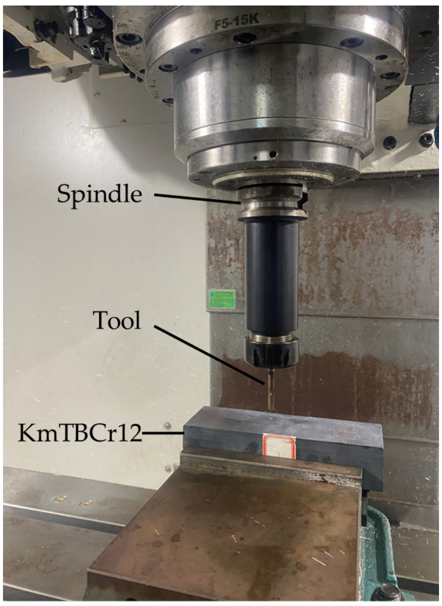

Figure 1. Schematic diagram of cutting.

Table 3. Chemical composition of KmTBCr12 (wt%).

Brand	C	Mn	Si	Ni	Cr	Mo	Cu	P	S
KmTBCr12	2.0–3.3	≤2.0	≤1.5	≤2.5	11.0–14.0	≤3.0	≤1.2	≤0.10	≤0.06

Table 4. Tool geometry and milling parameters.

Parameters	Values
Tool diameter (mm)	8
Milling flute number	4
Milling method	Forward milling
Cutting speed (mm/min)	85, 105, 125
Feed rate (mm/r)	0.2
Depth of cut (mm)	0.2
Cutting fluid	None

3. Results and Discussion

3.1. Microstructure and Mechanical Properties

The surface morphology of the coating obtained by SEM is shown in Figure 2a. There are microscopic defects such as white particles and pits on the surface of the coating; this is because, in the process of ion plating deposition, droplets splashed and adhered to the surface of the coating. The defects will seriously affect the surface quality of the coating, and the surface defects can be reduced by adjusting process parameters [26–28]. The elements of the AlTiZrN coating were scanned by EDS, and the distribution of each element is shown in Figure 2b. It can be seen from the figure that the distributions of the Al and Zr element are relatively uniform, while that of the Ti and N elements are relatively dispersed, which are related to the ratio of each component of the target and N_2 flow rate.

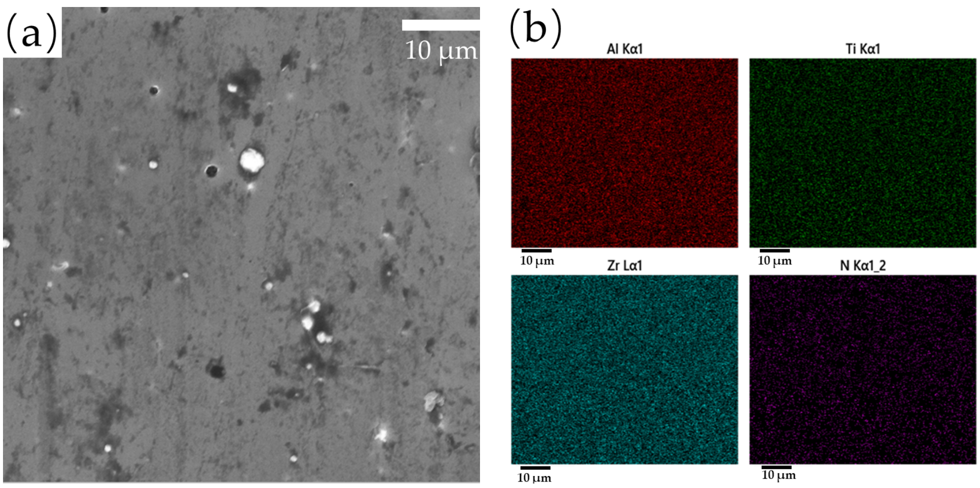

Figure 2. Surface morphology and element distribution of the coating: (**a**) surface morphology; (**b**) element distribution.

Figure 3 shows the XRD pattern of the AlTiZrN coating. The AlTiZrN coating shows a face-centered cubic (fcc) structure of TiN, with four diffraction peaks at 35.669°, 39.167°, 73.147°, and 75.530° corresponding to (111), (200), (311), and (222) respectively, and the diffraction peak at (111) is narrow and high. The XRD pattern was first fitted by Jade software, and then data analysis was used to obtain the full width at half maximum and lattice size of four diffraction peaks of 35.669°, 39.167°, 73.147°, and 75.530°. The specific values are shown in Table 5. When the diffraction peak is (111), the lattice size reaches 687 Å, and when the diffraction peak is (220), the lattice size is 158 Å, which indicates that grain refinement occurs at this time.

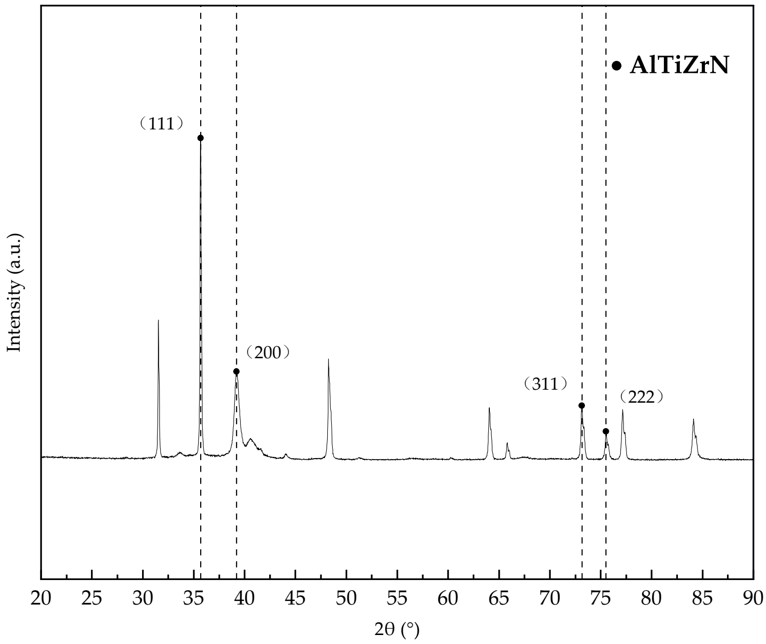

Figure 3. XRD pattern of the AlTiZrN coating.

Table 5. Diffraction peak FWHM and lattice size of the AlTiZrN coating.

Diffraction Peak	2θ	FWHM	Lattice Size (Å)
(111)	35.669°	0.157	687
(220)	39.167°	0.542	158
(311)	73.147°	0.234	467
(222)	75.530°	0.246	446

Uncoated tools and AlTiZrN-coated tools are shown in Figure 4a, and the colour of the AlTiZrN coating is golden yellow. The cross-sectional morphology of the AlTiZrN coating and substrate is shown in Figure 4b. The measured thickness of the coating was about 1.792 µm, and the coating was dense, well-bonded with the substrate, and had no obvious gap. There were some pits on the top of the coating caused by the uneven cutting of the sample. The chemical composition of the deposited coating was analyzed by the EDS software of the SEM. The results are shown in Table 6.

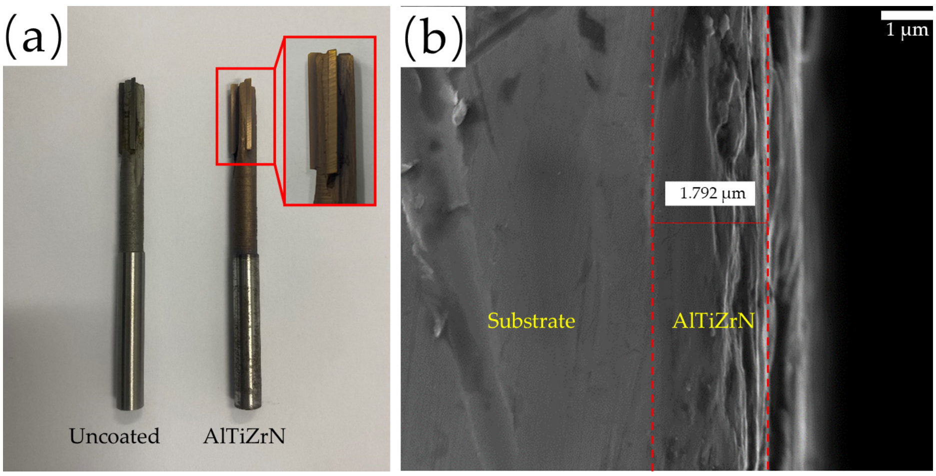

Figure 4. Cutting tool and section morphology: (**a**) uncoated and coated tools; (**b**) cross-sectional morphology.

Table 6. Chemical composition and mechanical properties of the coating.

Coating	Chemical Composition (at.%)				Thickness (μm)	Hardness ($HV_{0.05}$)	COF
	Al	Ti	Zr	N			
AlTiZrN	18.55	11.28	23.17	47.00	1.792	3887	0.32

The average hardness of the AlTiZrN coating measured by the Micro-Vickers hardness tester is 3887 $HV_{0.05}$. The hardness of the traditional AlTiN coating is 2800–3300 HV [29–31]. Doping Zr can improve the hardness of the AlTiN coating by at least 17.8%. Some studies had shown that when the percentage content of the Al, Ti, and Zr was close to 1:1:1, the possibility of the extreme hardness of the coating was greater [32,33].

For coated tools, the bonding strength between the coating and substrate will affect the cutting performance and life of the tools to a certain extent. Due to the complex shape of the tool, it is impossible to accurately measure the bonding strength of the coating. Therefore, this paper chose to use a Rockwell hardness tester to test the bonding strength of the coating on the surface of YG8 samples. Figure 5a shows the standard diagram for judging the bonding strength between the PVD coating and substrate. Under the HF1~HF4 standards, slight cracks were generated around the indentation opening, which is the qualified bonding strength. Under the HF5 and HF6 standards, the coating near the indentation opening was peeling, and the strength was unqualified. The indentation morphology of the AlTiZrN coating on the surface of the cemented carbide was observed by an optical microscope, as shown in Figure 5b. There are only cracks around the indentation, and the coating did not peel. By comparing the number and shape of cracks, it can be judged that the bonding strength between AlTiZrN coating and cemented-carbide substrate meets the HF3 standard.

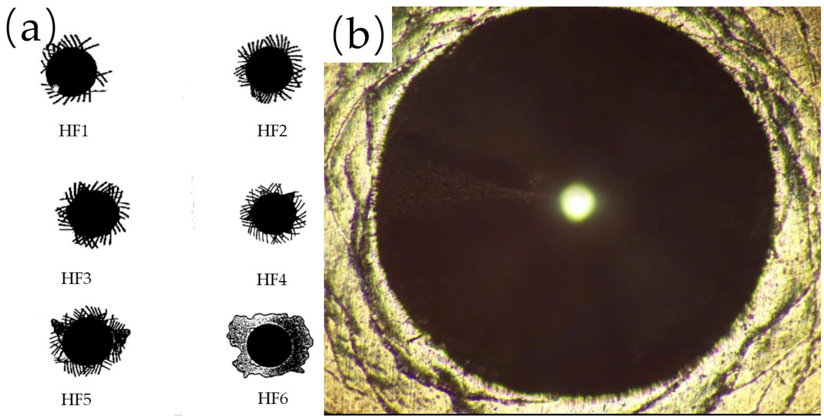

Figure 5. Bonding strength of the coating: (**a**) DB32/T 2945-2016 standard; (**b**) AlTiZrN coating indentation.

Coefficient of friction (COF) is another index to measure the mechanical properties of the coatings. For fine machining tools, the COF of the surface is the main parameter that reflects the cutting performance. The smaller the COF, the smaller the machining deformation of the tool, and the better the cutting ability when the cutting force is reduced. The COF curve of the AlTiZrN coating measured by the friction and wear tester is shown in Figure 6. The COF curve of the AlTiZrN coating fluctuates in the range of 0.2~0.4. After calculation, the average value of COF is 0.32. In [14], COF values of 0.65 were reported for AlTiN-TiSiN coating deposited on the nitrided tool steels. In [34], COF values between 0.62 and 0.68 were reported for AlCrN coatings deposited on HS6-5-2 steel substrates, and in [35], values of around 0.5–0.75 were reported for nanocomposite TiAlN coatings deposited on different steels. Therefore, the AlTiZrN coating prepared in this paper had a better COF.

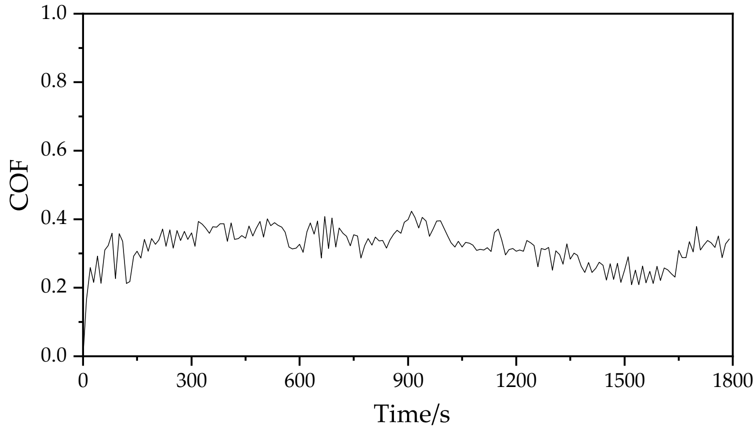

Figure 6. COF curve.

3.2. Cutting Performance

The flank wear curves of the uncoated and AlTiZrN-coated cemented-carbide tools at different cutting speeds are shown in Figure 7. At the cutting speed of 85 mm/min, the wear of the uncoated and coated tools can be divided into three stages. Within 0–9 cm, AlTiZrN-coated tools are in the initial wear stage, and the wear amount is small. With the increase of cutting length, the wear amount of the flank increases steadily, and the tool wears sharply after cutting 33 cm. When the cutting length is 36 cm, the wear width of the tool flank exceeds 0.1 mm, and the tool reaches the failure state. Through the curve, the cutting length of the tool can be calculated to be about 35.5 cm. However, the uncoated tool showed sharp wear after cutting 21 cm and finally reached the failure state when the cutting distance was 29.4 cm. When the cutting speed was 105 or 125 mm/min, the flank wear did not increase slowly, and the wear curve of the uncoated tool was steeper than that of the coated tool. Finally, the cutting length of the uncoated and coated cemented-carbide tools was 20.5 and 25.1 cm, respectively, at the speed of 105 mm/min; At the speed of 125 mm/min, the cutting lengths of the uncoated and AlTiZrN-coated cemented-carbide tools were 14.5 and 19.6 cm, respectively. Comparing the flank wear curve, it can be seen that the wear stage of the AlTiZrN-coated cemented-carbide tools is more obvious and stable under three different cutting speeds, which proves that AlTiZrN-coated cemented-carbide tools have less wear in cutting than uncoated tools.

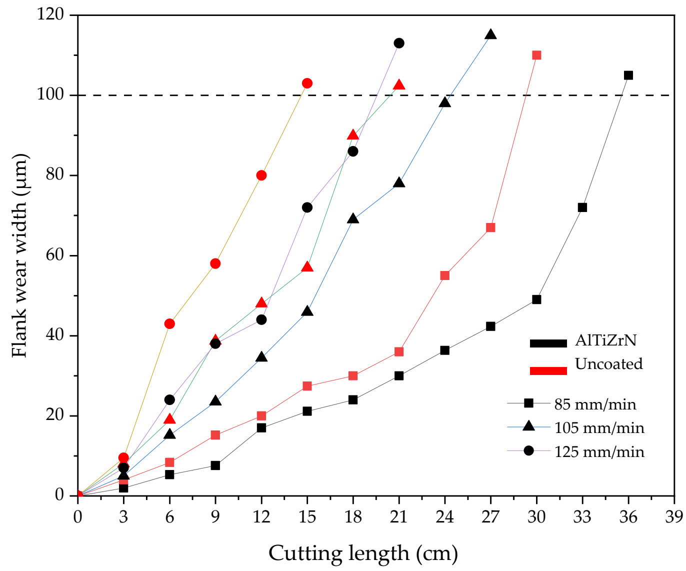

Figure 7. Relationship between flank wear and cutting length of the uncoated and AlTiZrN-coated tools at different cutting speeds.

Figure 8 shows the cutting length of the uncoated tool and AlTiZrN-coated tool at different cutting speeds. With the increase in cutting speed, the lives of both types of tools will be greatly shortened. At the cutting speeds of 85, 105, and 125 mm/min, the lives of the AlTiZrN-coated tools are increased by 20.7%, 22.4%, and 35.2%, respectively. The data shows that under the condition of high-speed cutting, the coated tools had more advantages than the uncoated tools.

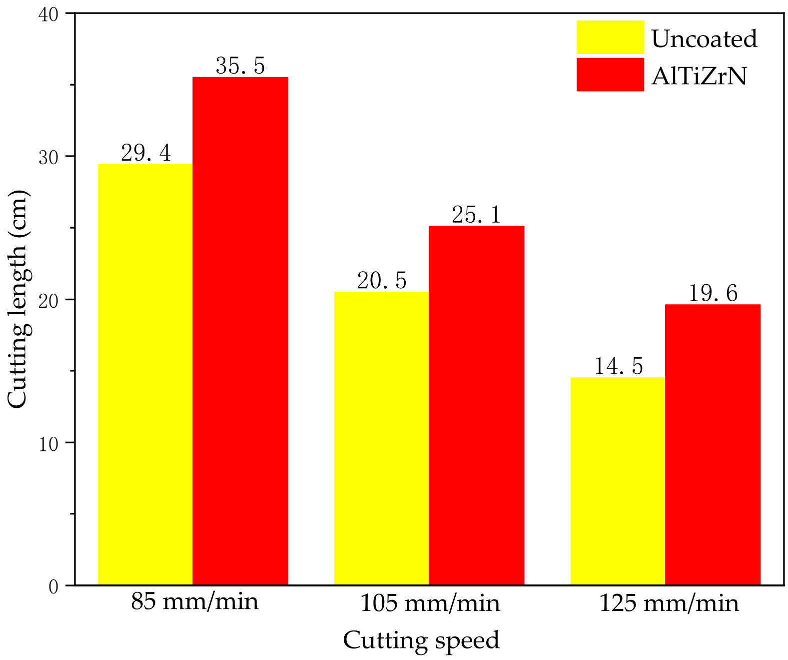

Figure 8. Cutting length of the uncoated and AlTiZrN-coated tools at different cutting speeds.

3.3. Wear Mechanism

Figure 9 shows the relationship between flank wear and cutting length of an uncoated tool and an AlTiZrN-coated tool at different wear stages at a cutting speed of 125 mm/min. In the early stage of the cutting process, the wear of the two kinds of tools was relatively uniform, which was simple flank wear, and the uncoated tool wore down at a greater rate at the same cutting distance. With the increase in cutting distance, the cutting edge of the tool gradually dulled. When the cutting distance was 9 cm, the micro-edge collapse of the two kinds of tools occurred, which led to a decline in cutting performance [36].

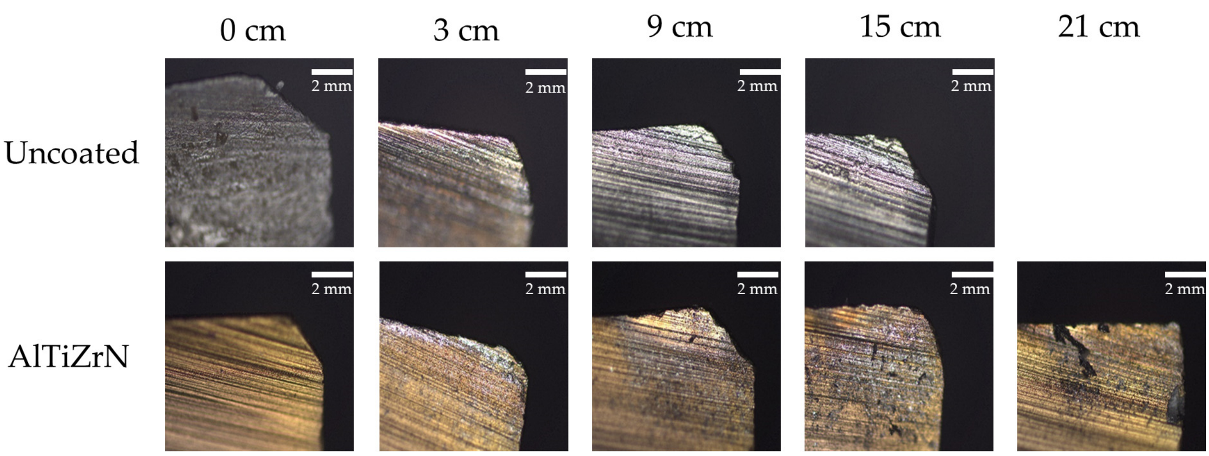

Figure 9. Flank wear image of the uncoated tool and AlTiZrN-coated tool when the cutting speed is 125 mm/min.

Because the uncoated tool had no coating protection, it led to large-area wear on the flank, which accelerated the failure of the tool. When the cutting distance was increased to 15 cm, the uncoated tool reached the failure standard, and a large number of cutting edges collapsed. The small pits and grooves on the flank of the AlTiZrN-coated tool are due to the existence of small particles with high hardness in the workpiece material. During the process of cutting, the small particles rub against the rotating tool, and this will lead to defects on the flank. When the cutting distance reached 21 cm, due to periodic impact and alternating thermal stress, the AlTiZrN coating peeled off, and obvious cracks and grooves appeared on the flank. By analyzing the wear morphology of the flank, it can be seen that the wear resistance of the AlTiZrN-coated tools is better than that of the uncoated tools.

In order to study the wear failure form of the flank of the AlTiZrN-coated tool, the coated tools with the cutting length of 9 and 15 cm, respectively at the speed of 125 mm/min are selected. The cemented-carbide tool was cut by a wire-cutting machine, and a small part was intercepted for EDS analysis. Figure 10 shows the results of EDS. In the middle stage of tool wear, the content of the Al, Ti, Zr, and N in the surface layer of coated tool flank was lower than that of the coating, and slight friction and wear occurred. At the same time, a small amount of Fe and O elements appear. Because the coating and cemented-carbide did not contain Fe and O elements, it indicates that a small amount of high-chromium cast iron adhered to the back surface of the tool at this time, and an oxidation reaction occurred. At this time, the wear forms are slight bonding wear and oxidation wear. In the later stage of cutting, a large number of Fe and O elements, as well as an appropriate amount of Cr, a small amount of Ni, and trace Si elements begin to appear on the flank of the coated tool. The constituent elements of the AlTiZrN coating are greatly reduced, the cutting part of the tool contacts and rubs against the chip, and some hard spots of the workpiece material will be taken away by the tool. At this time, the wear mechanisms of the flank of the tool are serious oxidation wear and bonding wear. Therefore, the wear mechanism of the AlTiZrN coating in high-speed cutting includes friction wear, oxidation wear, and bonding wear, among which the oxidation wear and bonding wear are the main wear forms. The wear mechanisms of the AlTiZrN-coated tools are similar to that of the AlTiN- and TiAlSiN-coated tools in reference [31].

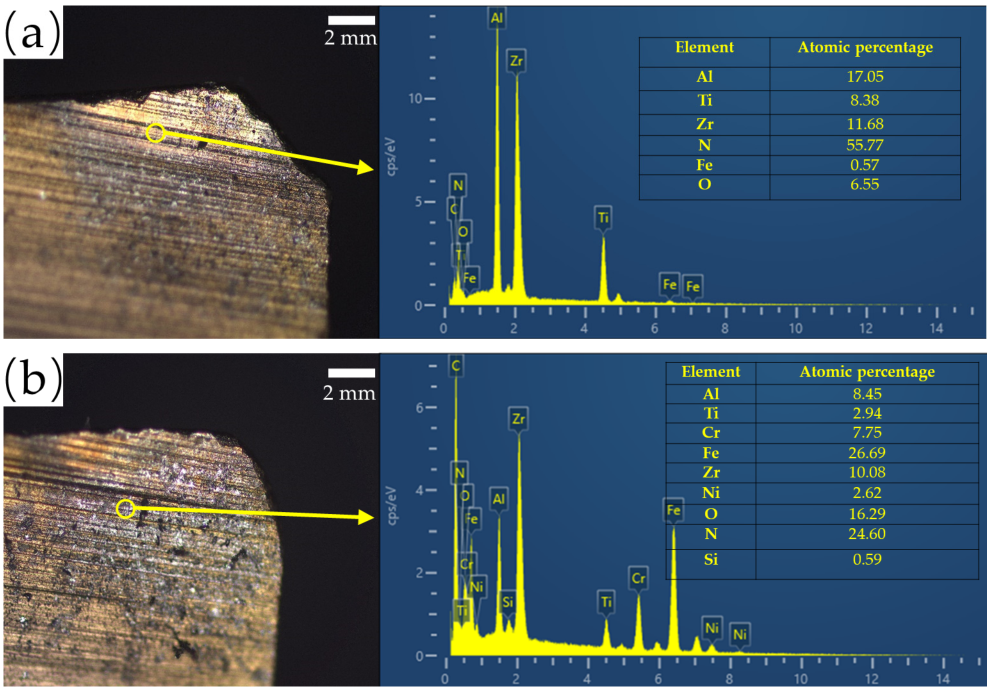

Figure 10. EDS analysis of the flank surface of the AlTiZrN-coated tools at a speed of 125 mm/min: (**a**) the cutting length is 9 cm; (**b**) the cutting length is 15 cm.

3.4. Chip Formation

Under different cutting conditions, the shapes of chips produced by cutting KmTBCr12 are also different. Figure 11 shows the chips produced by the uncoated tools and AlTiZrN-coated tools when the cutting length was 9 cm at the speed of 125 mm/min. The chips produced by the two kinds of tools are curled, but the chips produced by coated tools are generally shorter, which indicates that the coated tools have a better chip-breaking performance than the uncoated tools, and the coated tools are more suitable for cutting. Figure 11c,d shows the machining path of the tool on the workpiece surface. Combined with the wear diagram of the flank in Figure 9, it can be seen that the wear of the coated tool was relatively slight, the scratches were more uniform and smooth, and the surface quality of the workpiece was good. The cutting edge of the uncoated tools was seriously worn, the scratches were more rough and uneven, and the surface of the workpiece was rough. Therefore, it can be judged that under the same conditions, the coated tool has better chip-breaking performance and good machining surface quality.

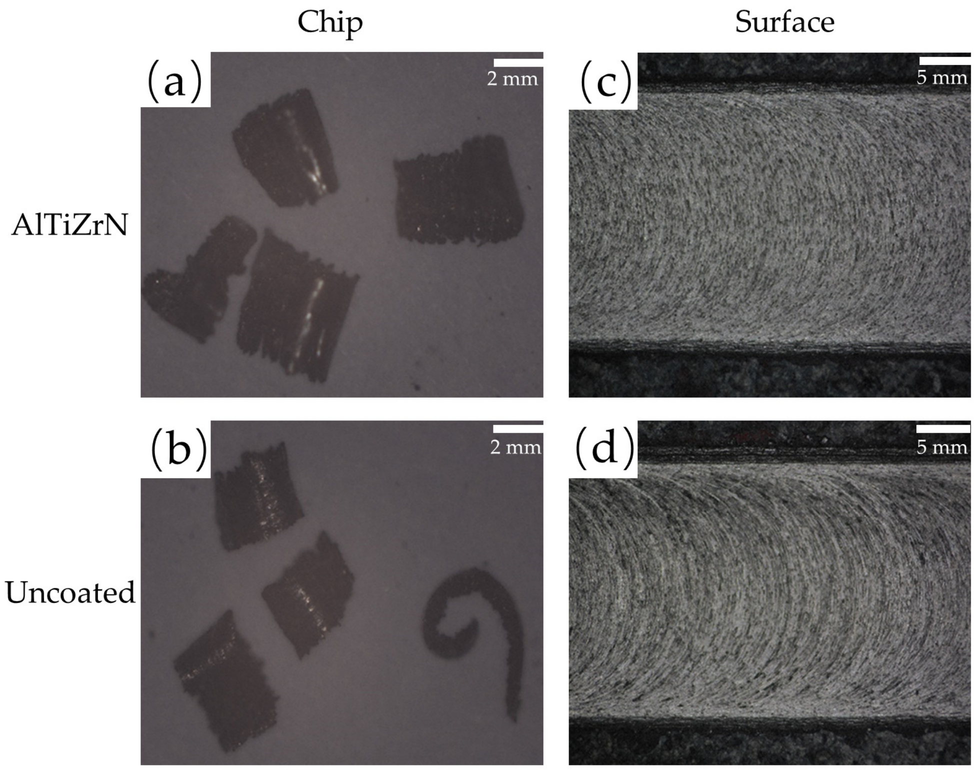

Figure 11. Chip and machining path produced by the tools when the cutting speed is 125 mm/min and the cutting length is 9 cm: (**a**,**c**) AlTiZrN-coated tools; (**b**,**d**) uncoated tools.

Figure 12 shows the chip and machining path generated by the AlTiZrN-coated tool when the cutting length was 9 cm at different cutting speeds. It can be seen from the figure that when the cutting speed was low, the generated chips were bent and long; the scratches formed by tool machining were not uniform, and the surface was rough. With the increase in cutting speed, the chips gradually became smaller, and the scratches tended to be uniform and smooth, indicating that the chip-breaking performance of the tool improved at this time. Therefore, under the relatively high-speed cutting conditions, the chip-breaking performance of the AlTiZrN coating was also better.

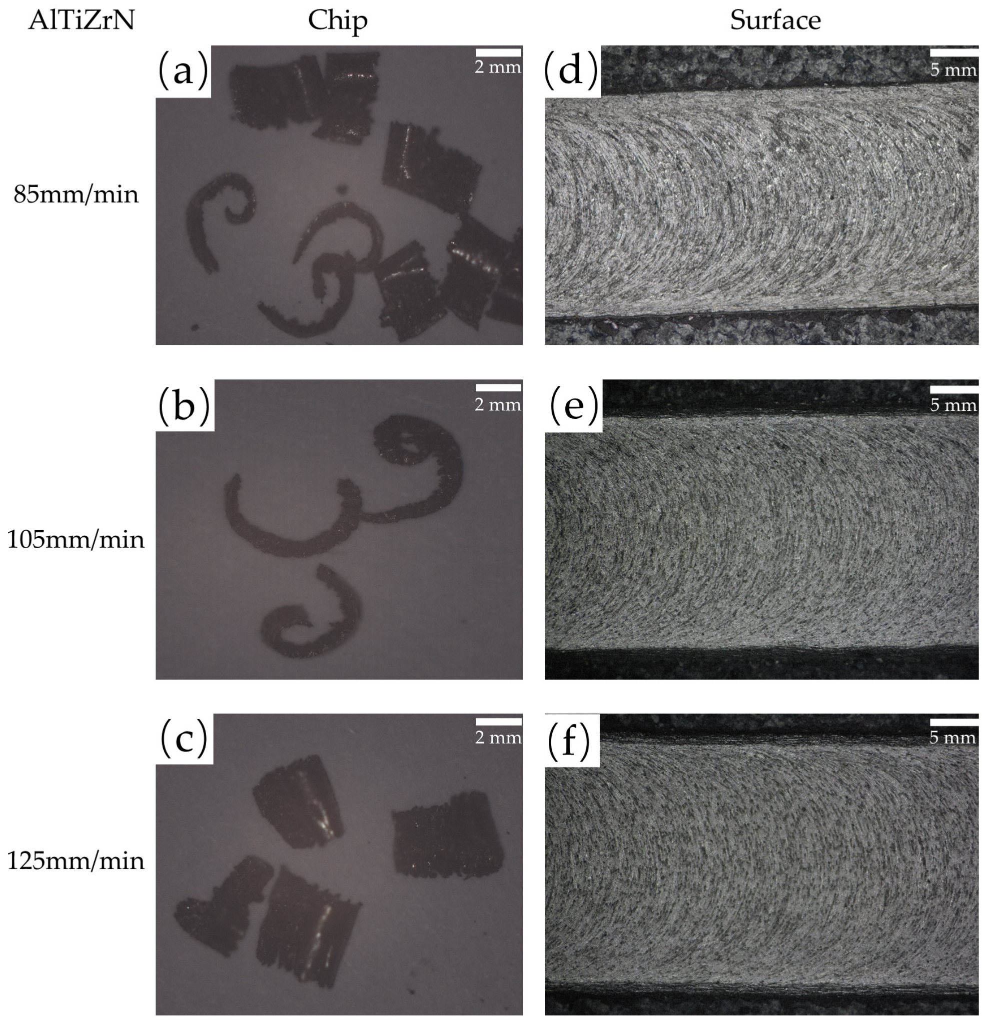

Figure 12. When the cutting length is 9 cm, the chips and machining path produced by the AlTiZrN-coated tools at different cutting speeds. (**a**,**d**) 85 mm/min; (**b**,**e**) 105 mm/min; (**c**,**f**) 125 mm/min.

4. Conclusions

Based on the above research on the preparation of a cemented-carbide AlTiZrN-coated tool and its wear behavior during dry-milling of high-chromium cast iron KmTBCr12, the following conclusions can be obtained:

1. The AlTiZrN coating presents the fcc structure of TiN; The average microhardness is 3887 $HV_{0.05}$. Compared with the traditional high hardness AlTiN coating, the hardness is increased by at least 17.8%. Higher hardness will improve the wear resistance of the tool. The bonding strength between the coating and the substrate meets the standard HF3 and is up to the requirements. The COF of the coating is about 0.32. Compared with AlTiN, AlCrN, and other coatings, the COF is smaller, and the cutting performance is better.
2. The AlTiZrN coating can significantly improve the life of the cemented-carbide tool. At the cutting speeds of 85, 105, and 125 mm/min, the lives of the AlTiZrN-coated tools are increased by 20.7%, 22.4%, and 35.2%, respectively, compared with uncoated tools. Under the same cutting condition, AlTiZrN-coated tools have better cutting and chip-breaking performance than uncoated tools. With the increase in cutting speed, the workpiece chips produced by the AlTiZrN-coated tools are smaller and more uniform, and the scratches on the machined surface are smoother. Therefore, at a higher cutting speed, the AlTiZrN-coated tools have more advantages in the life and cutting performance than that of the uncoated tools.

3. During the cutting process, the wear mechanisms of the AlTiZrN-coated tools mainly include friction, oxidation, and bonding, while oxidation and bonding wear are the main wear mechanisms in the later stage of wear. The main wear mechanisms of the AlTiN- and TiAlSiN-coated tools include bonding, diffusion, oxidation, and cracks. In contrast, the AlTiZrN-coated tools have more advantages in terms of wear.

Author Contributions: Conceptualization, H.Y.; methodology, H.Y., R.W. and Z.G.; formal analysis, R.L. and S.W.; investigation, R.L.; resources, R.L. and S.W.; data curation, H.Y.; writing—original draft preparation, H.Y.; writing—review and editing, R.W., Z.G., R.L., S.W. and J.W.; supervision, R.L.; funding acquisition, R.L. and S.W. All authors have read and agreed to the published version of the manuscript.

Funding: This research was funded by the University–Industry Cooperation Project of Fujian Province (Grant No. 2021H6031), the Collaborative Special Project for Fuxia-Quan Autonomous Region (Grant No. 3502ZCQXT2021004), the Major Science and Technology Project of Xiamen City (Grant No. 3502Z20191022) and the Educational Research Project for Young and Middle-aged Teachers of Fujian Province (Grant No. JAT210253).

Institutional Review Board Statement: Not applicable.

Informed Consent Statement: Not applicable.

Data Availability Statement: Not applicable.

Conflicts of Interest: The authors declare no conflict of interest.

References

1. Fortini, A.; Suman, A.; Vulpio, A.; Merlin, M.; Pinelli, M. Microstructural and Erosive Wear Characteristics of a High Chromium Cast Iron. *Coatings* **2021**, *11*, 490. [CrossRef]
2. Deng, J.; Zhou, J.; Zhang, H.; Pei, Y. Wear mechanisms of cemented carbide tools in dry cutting of precipitation hardening semi-austenitic stainless steels. *Wear* **2011**, *270*, 520–527. [CrossRef]
3. Fan, Y.; Hao, Z.; Zheng, M. Wear characteristics of cemented carbide tool in dry-machining Ti-6Al-4V. *Mach. Sci. Technol.* **2016**, *20*, 249–261. [CrossRef]
4. Huang, Y.; Chou, Y.K.; Liang, S.Y. CBN tool wear in hard turning: A survey on research progresses. *Int. J. Adv. Manuf. Technol.* **2007**, *35*, 443–453. [CrossRef]
5. Wang, Z.; Rahman, M.; Wong, Y. Tool wear characteristics of binderless CBN tools used in high-speed milling of titanium alloys. *Wear* **2005**, *258*, 752–758. [CrossRef]
6. Kumar, P.; Chauhan, S.R.; Pruncu, C.I.; Gupta, M.K.; Pimenov, D.Y.; Mia, M.; Gill, H.J. Influence of Different Grades of CBN Inserts on Cutting Force and Surface Roughness of AISI H13 Die Tool Steel during Hard Turning Operation. *Materials* **2019**, *12*, 177. [CrossRef] [PubMed]
7. Guo, C.; Wang, A.; Wang, Z.; Chen, H. Study on Optimization of cutting tools and cutting parameters in cutting high chromium cast iron. *Mod. Manuf. Eng.* **2009**, *10*, 69–71. [CrossRef]
8. Fan, Q.; Lin, J.; Wang, T. Latest research progress of tool coating materials. *Surf. Technol.* **2022**, *51*, 1–19. [CrossRef]
9. Qin, Z.; Xian, G.; Zhao, H.; Zheng, Y.; Fan, H.; Wang, J. Research status and future development of TiCN coatings deposited on cutting tools. *Surf. Technol.* **2016**, *45*, 125–133. [CrossRef]
10. Shen, T.; Zhu, L. Comparison of microstructure and properties between TiN/TiCN/Al_2O_3/TiN and TiN/TiCN/Al_2O_3/TiCNO multilayer coatings. *Surf. Technol.* **2020**, *49*, 141–148. [CrossRef]
11. Li, Y.; Chen, X.; Xu, Y.; Lin, J.; Gao, Y.; Wen, G. Research on growth way of Al_2O_3 and TiCN coating on cemented carbide. *Cem. Carbide* **2015**, *32*, 147–154.
12. Alamgir, A.; Bogatov, A.; Jõgiaas, T.; Viljus, M.; Raadik, T.; Kübarsepp, J.; Sergejev, F.; Lümkemann, A.; Kluson, J.; Podgursky, V. High-Temperature Oxidation Resistance and Tribological Properties of Al_2O_3/ta-C. *Coat. Coat.* **2022**, *12*, 547. [CrossRef]
13. Wei, S.; Lu, P.; Lin, R. Surface coating tools of TiAlN technology application to machining. *Eng. J. Wuhan Univ.* **2014**, *47*, 703–706.
14. Claver, A.; Randulfe, J.J.; Palacio, J.F.; Fernández de Ara, J.; Almandoz, E.; Montalá, F.; Colominas, C.; Cot, V.; Garcia, J.A. Improved Adhesion and Tribological Properties of AlTiN-TiSiN Coatings Deposited by DCMS and HiPIMS on Nitrided Tool Steels. *Coatings* **2021**, *11*, 1175. [CrossRef]
15. Gil, D.; Veiga, F.; Pereira, O.; Lopez De Lacalle, L.N. Threading Performance of Different Coatings for High Speed Steel Tapping. *Coatings* **2020**, *10*, 464. [CrossRef]
16. Chowdhury, S.; Bose, B.; Yamamoto, K.; Veldhuis, S.C. Effect of Interlayer Thickness on Nano-Multilayer Coating Performance during High Speed Dry Milling of H13 Tool Steel. *Coatings* **2019**, *9*, 737. [CrossRef]
17. Wang, R.; Yang, H.; Guo, Z.; Wei, S.; Lin, R. Study on the Cutting Performance of CrN/AlCrN-Coated Carbide PCB Milling Cutter. *Coatings* **2022**, *12*, 556. [CrossRef]

18. De Almeida, E.A.S.; Milan, J.C.G.; da Costa, C.E.; Binder, C.; de Mello, J.D.B.; Costa, H.L. Combined Use of Surface Texturing, Plasma Nitriding and DLC Coating on Tool Steel. *Coatings* **2021**, *11*, 201. [CrossRef]
19. Grigoriev, S.N.; Volosova, M.A.; Fedorov, S.V.; Migranov, M.S.; Mosyanov, M.; Gusev, A.; Okunkova, A.A. The Effectiveness of Diamond-like Carbon a-C:H:Si Coatings in Increasing the Cutting Capability of Radius End Mills When Machining Heat-Resistant Nickel Alloys. *Coatings* **2022**, *12*, 206. [CrossRef]
20. Zheng, S.; Sun, D. Experimental study on cutting performance and wear resistance of DLC coated milling cutter. *J. Chongqing Univ. Sci. Technol.* **2021**, *23*, 50–53. [CrossRef]
21. Ekroth, M.; Frykholm, R.; Lindholm, M.; Andrén, H.-O.; Ågren, J. Gradient zones in WC-Ti(C,N)-Co-based cemented carbides: Experimental study and computer simulations. *Acta. Mater.* **2000**, *48*, 2177–2185. [CrossRef]
22. Vereschaka, A.; Milovich, F.; Andreev, N.; Sitnikov, N.; Alexandrov, I.; Muranov, A.; Mikhailov, M.; Tatarkanov, A. Efficiency of Application of (Mo, Al)N-Based Coatings with Inclusion of Ti, Zr or Cr during the Turning of Steel of Nickel-Based Alloy. *Coatings* **2021**, *11*, 1271. [CrossRef]
23. Wu, J.; Li, Z.; Peng, L.; Yong, Y.; Zhang, J. Effect of nitrogen partial pressure on the structure and color of ZrN films. *Vacuum* **2021**, *58*, 57–62. [CrossRef]
24. Zhang, J.; Peng, L.; Wang, X.; Liu, D.; Wang, N. Effects of Zr/(Zr+Ti) Molar Ratio on the Phase Structure and Hardness of TixZr1−xN Films. *Coatings* **2021**, *11*, 1342. [CrossRef]
25. Yan, X.; Zhang, J.; Yu, Y. Deposition Process and Properties of TiN and ZrN Films Coated on Stainless Steel Root Canal Files. *Surf. Technol.* **2019**, *48*, 294–301. [CrossRef]
26. Wei, Y.; Hou, J.; Jiang, Z.; Tian, X. Research status of removal methods for macroparticles defects in arc ion plating process. *Hot Work. Technol.* **2016**, *45*, 28–32. [CrossRef]
27. Wei, Y.Q.; Li, C.W.; Gong, C.Z.; Tian, X.-B.; Yang, S.-Q. Microstructure and mechanical properties of TiN/TiAlN multilayer coatings deposited by arc ion plating with separate targets. *Trans. Nonferrous Met. Soc. China* **2011**, *21*, 1068–1073. [CrossRef]
28. Dong, X.; Zhang, Z.; Liang, H.; Bian, C.; Huang, N.; Huang, X. Research on reducing macroparticles during arc ion plating. *Heat Treat. Met.* **2012**, *37*, 125–127. [CrossRef]
29. Rui, W.; Mei, H.-J.; Li, R.-S.; Zhang, Q.; Zhang, T.-F.; Wang, Q.-M. Friction and wear behavior of AlTiN-Coated carbide balls against SKD11 hardened steel at elevated temperatures. *Acta Metall. Sin.* **2018**, *31*, 1073–1083. [CrossRef]
30. Wu, Y.; Wang, L.; Chen, Q.; Huang, B.; Zhang, E.; Zhou, Q.; Zheng, G. Properties and milling performance of AlTiN and TiAlSiN coatings prepared by cathodic arc. *China Ceram.* **2019**, *55*, 29–35. [CrossRef]
31. Liu, J.; Zhu, S.-S.; Deng, X.; Liu, J.-Y.; Wang, Z.-P.; Qu, Z. Cutting performance and wear behavior of AITiN-and TiAlSiN-Coated carbide tools during dry milling of Ti-6Al-4V. *Acta Metall. Sin.* **2020**, *33*, 459–470. [CrossRef]
32. Zhang, C. Investigation on Influence Factors and Distribution Law of Hardness of TiAlZrN Film System. Master's Thesis, Shenyang University, Shenyang, China, 2021.
33. Li, C.; Holec, D.; Du, Y.; Mayrhofer, P.H. Influence of Zr on structure, mechanical and thermal properties of Ti-Al-N. *Thin Solid Film.* **2011**, *519*, 5503–5510. [CrossRef]
34. Warcholinski, B.; Gilewicz, A.; Myslinski, P.; Dobruchowska, E.; Murzynski, D. Structure and properties of AlCrN coatings deposited using cathodic arc evaporation. *Coatings* **2020**, *10*, 793. [CrossRef]
35. Al-Bukhaiti, M.A.; Al-Hatab, K.A.; Tillmann, W.; Hoffman, F.; Sprute, T. Tribological and mechanical properties of Ti/TiAlN/TiAlCN nanoscale multilayer PVD coatings deposited on AISI H11 hot work tool steel. *Appl. Surf. Sci.* **2014**, *318*, 180–190. [CrossRef]
36. Liu, H.; Wang, M.; Liu, X. Research on wear performance of composite coating tool drilling Inconel 718. *Agric. Equip. Veh. Eng.* **2022**, *60*, 65–69.